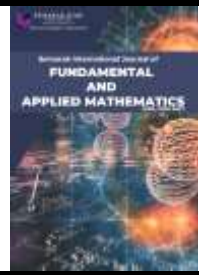




Semarak International Journal of Fundamental and Applied Mathematics

Journal homepage:
<https://semarakilmu.my/index.php/sijfam>
ISSN: 3030-5527



Jeffrey Fluid Flow over a Stretching Sheet with Microrotation Effect under Convective Boundary Condition

Nur Syamilah Arifin^{1,*}, Syazwani Mohd Zokri², Abdul Rahman Mohd Kasim³

¹ College of Computing, Informatics and Mathematics, Universiti Teknologi MARA Johor Branch Pasir Gudang Campus, Jalan Purnama, Bandar Seri Alam, 81750, Masai, Johor, Malaysia

² College of Computing, Informatics and Mathematics, Universiti Teknologi MARA Kuala Terengganu Branch, Kuala Terengganu Campus, 21080, Kuala Terengganu, Malaysia

³ Centre for Mathematical Sciences, Universiti Malaysia Pahang Al-Sultan Abdullah (UMPSA), Lebuhr Persiaran Tun Khalil Yaakob, 26300 Kuantan, Pahang, Malaysia

ARTICLE INFO

Article history:

Received 20 December 2024

Received in revised form 23 January 2025

Accepted 25 February 2025

Available online 15 March 2025

Keywords:

Jeffrey micropolar fluid; convective boundary condition

ABSTRACT

This paper investigates the flow and heat transfer of Jeffrey micropolar fluid across a stretching sheet with the effect of convective boundary conditions. The governing boundary layer equation in the form of partial differential equations are transformed into ordinary differential equations and solved numerically using RKF45 approach by Maple Software. The effects of Prandtl number, Deborah number, velocity slip, material parameter, Biot number, concentration of microelement and stretching parameter on the velocity, microrotation and temperature profiles as well as skin friction coefficients and the local Nusselt number are presented and discussed. There is excellent agreement between the current and previously published data. The results revealed that as Pr increases, the boundary layer becomes thinner and reduces the temperature. The effect of Deborah number are increased the relaxation time and velocity while increasing the velocity slip parameter k , concentration of microelements, stretching stretch parameter and Biot number increases the heat transfer coefficient which improves the fluid's temperature as well as the thickness of its thermal boundary layer. It has been discovered that increasing material parameter K causes a decrease in fluid velocity while for microrotation profiles K gradually increases until one maximum value and then gradually decreases until it is asymptotically zero.

1. Introduction

The study of non-Newtonian fluids continues to be a hot issue. The unique characteristics of non-Newtonian fluids in pharmaceuticals, physiology, fibers technology, food products, wire coating, crystal growth, and other fields have generated interest in this field of research. Several research of non-Newtonian fluids in various geometries have been carried out due to the practical and fundamental relation of these fluids to industrial applications.

* Corresponding author.

E-mail address: nursyamilaharifin@uitm.edu.my

<https://doi.org/10.37934/sijfam.5.1.3543b>

In an asymmetric channel, Nadeem *et al.*, [1] demonstrated the peristaltic flow of a Jeffrey fluid with changing viscosity. Khan *et al.*, [2] documented some unsteady Jeffrey fluid flows between two side walls over a plane wall, whereas Hayat *et al.*, [3] studied the boundary layer flow of a Jeffrey fluid with the influence of convective boundary conditions. Hayat *et al.*, [4] also discusses the effects of thermal radiation endoscope and magnetic field on the mixed convection stagnation point flow of Jeffery fluid. In addition, research activities on magnetic field flow under various circumstances have been discovered by several authors [5,6].

Vajravelu *et al.*, [7] on the other hand, investigated the impact of heat transfer on the peristaltic transport of Jeffrey fluid in a vertical porous stratum. Turkyilmazoglu and Pop [8] found an exact numerical model for flow and heat transmission around the stagnation point on a stretching/shrinking sheet. Zin *et al.*, [9] analyzed the effect of Newtonian heating and thermal radiation on the combined heat and mass transfers for an unstable free convection MHD flow of Jeffrey fluid through an oscillating vertical plate. Another study by

Although many publications have been focused on the Jeffrey fluid: however, the numerical solution considering the microrotation effect is very scarce. Eringen [10] established the theory of micropolar fluid, which includes microscopic characteristics such as microrotation and rotational inertia of microelements and belongs to the class of non-symmetric stress tensors. This theory is capable of explaining the deformation of complex engineering structures, whereas the Navier–Stokes model is incapable to explain [11]. Micropolar fluid is a subset of Eringen's micromorphic fluid theory, which he introduced first. This fluid is designed to simulate fluids with hard randomly oriented particles suspended in a viscous medium with an important micro motion in rotation. Colloidal fluids, biological fluids in thin vessels and polymeric suspensions are examples of micropolar fluids in real life [12].

Most previous studies were specifically directed to Jeffrey fluid only, whereas very few were found to include the microrotation effect. Therefore, the present study aims to explore the Jeffrey fluid flow over a stretching sheet with microrotation effect under convective boundary condition. The governed partial differential equations (PDEs) are reduced to ordinary differential equations ODEs by applying the similarity transformation variables. The resulting ODEs will be tackled via Runge-Kutta Fehlberg Method encoded in Maple software.

2. Problem Formulation

Consider the steady two-dimensional flow over a stretching sheet submerged in an incompressible and electrically conducting Jeffrey fluid at ambient temperature T_∞ . The rectangular Cartesian coordinates (x, y) are applied with the x and y axes being measured parallel to and normal to the plate, respectively, and the fluid occupying the region $y \geq 0$. A uniform magnetic field of strength B_0 is applied normal to the stretching sheet and directed in the positive y direction. Since the magnetic Reynolds number is considered to be small, the induced magnetic field is negligible. Figure 1 illustrates the physical model and coordinate system of this problem.

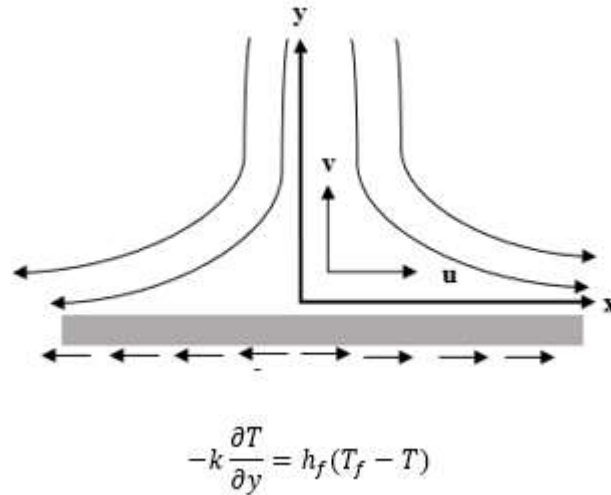


Fig. 1. Physical model of the coordinate system

The PDEs involving the continuity, momentum, microrotation and energy can be expressed as follows:

$$\frac{\partial u}{\partial x} + \frac{\partial v}{\partial y} = 0 \quad (1)$$

$$u \frac{\partial u}{\partial x} + v \frac{\partial u}{\partial y} = \frac{v + \frac{\kappa}{\rho}}{1 + \lambda_1} \left[\frac{\partial^2 u}{\partial y^2} + \lambda_2 \left(u \frac{\partial^3 u}{\partial x \partial y^2} - \frac{\partial u}{\partial x} \frac{\partial^2 u}{\partial y^2} + \frac{\partial u}{\partial y} \frac{\partial^2 u}{\partial x \partial y} + v \frac{\partial^3 u}{\partial y^3} \right) \right] + u_e \frac{\partial u_e}{\partial x} + \frac{\kappa}{\rho} \frac{\partial N}{\partial y} \quad (2)$$

$$u \frac{\partial N}{\partial x} + v \frac{\partial N}{\partial y} = \frac{\gamma}{\rho j} \frac{\partial^2 N}{\partial y^2} - \frac{\kappa}{\rho j} \left(2N + \frac{\partial u}{\partial y} \right) \quad (3)$$

$$u \frac{\partial T}{\partial x} + v \frac{\partial T}{\partial y} = \frac{k^*}{\rho c_p} \frac{\partial^2 T}{\partial y^2} \quad (4)$$

subject to boundary conditions:

$$\begin{aligned} u &= cx + g_x \frac{\partial u}{\partial y}, \quad v = 0, \quad N = -n \frac{\partial u}{\partial y}, \quad -k \frac{\partial T}{\partial y} = h_f(T_f - T) \text{ at } y = 0 \\ u &= u_e, \quad N \rightarrow 0, \quad \frac{\partial u}{\partial y} \rightarrow 0, \quad T \rightarrow T_\infty \text{ as } y \rightarrow \infty \end{aligned} \quad (5)$$

where u and v are the velocity components along the x and y -axes, ν is the kinematic viscosity, κ is a vortex viscosity, ρ is the fluid density, u_e is the velocity outside the boundary layer, N is the component of microrotation vector normal to the x and y -axes, γ the spin gradient, $j = \nu/a$ is the microinertia density, a is an arbitrary constants, T is the temperature, k^* is the thermal conductivity, c_p is the specific heat capacity, c is an arbitrary constants, g_x is slip constant depending on the λ_1 and n is the concentration of microelements in the range of $0 \leq n \leq 1$ respectively. Here, $n = 0$ indicates the concentrated particle flows in which the microelements close to the wall surface are unable to rotate ($N = 0$). The disappearance of the anti-symmetric component of the stress tensor is represented by $n = \frac{1}{2}$ which is referred as the weak concentration. γ is defined as

$$\gamma = \left(\mu + \frac{\kappa}{2} \right) j = \mu \left(1 + \frac{\kappa}{2} \right) j \quad (6)$$

where μ is a dynamic viscosity and $K = \kappa/\mu$ is denoted as material parameter. The following similarity transformation variables are introduced to the Eq. (1)-(5).

$$\eta = y\sqrt{\frac{c(1+\lambda_1)}{v}}, \quad u = cx\frac{\partial f}{\partial \eta}, \quad v = -\sqrt{\frac{cv}{1+\lambda_1}}f(\eta), \quad N = cx\sqrt{\frac{c(1+\lambda_1)}{v}}g(\eta), \quad \theta = \frac{T-T_\infty}{T_f-T_\infty} \quad (7)$$

The resulting equations can then be expressed as

$$f'' - f''' = (1 + \frac{k}{\mu})[f'''' + \beta(f'''' + f^5)] + \delta^2 + \frac{k}{\mu}(g') - f'' + f''' + (1 + K)[f'''' + \beta(f'''' + f^5)] + \delta^2 + K(g') = 0 \quad (8)$$

$$(1 + \frac{K}{2})g'' + fg' - f'g - K(2g + f'') = 0 \quad (9)$$

$$\theta'' + Prf\theta' = 0 \quad (10)$$

where the transformed boundary conditions take the following form:

$$f(0) = 0, \quad f' = 1 + kf''(\eta), \quad g(\eta) = -nf''(\eta), \quad \theta' = -Bi(1 - \theta) \text{ at } \eta = 0 \\ f' \rightarrow \delta, \quad f'' \rightarrow 0, \quad g \rightarrow 0, \quad \theta \rightarrow 0 \text{ as } \eta \rightarrow \infty \quad (11)$$

3. Result and Discussion

The resulting equations (8)–(11) are solved numerically by using the RKF45 method encoded in Maple software. The numerical analysis is presented graphically on the velocity $f'(\eta)$, microrotation profiles $g(\eta)$ and temperature profiles $\theta'(\eta)$ to investigate the various parameters of Prandtl number, Deborah number, velocity slip, material parameter, Biot number, concentration of microelement and stretching parameter. The results of this research are first validated by comparing them with the previously published study as shown in Table 1. For various values of Prandtl number Pr , the presented heat transfer $-\theta'(\eta)$ results are compared with Turkiymazoglu and Pop [8] and Rawi *et al.*, [12]. The table clearly shows that the comparison values are in a strong agreement. As a result, it is possible to conclude that the RKF45 method is effective, and the results presented in this study are accurate and reliable.

Table 1

Comparative values of heat transfer coefficient $-\theta'(0)$ for various values of Prandtl number Pr when $K = 0, k = 0, n = 0, \beta = 2, \delta = 1, Bi \rightarrow \infty, blt = 12$

Pr	Turkiymazoglu and Pop [8]	Rawi <i>et al.</i> , [12]	Present results
2	1.12837917	1.128732	1.12834543
5	1.78412412	1.785519	1.78405347
10	2.52313252	2.527078	2.52305404

Figures 1 - 10 show the distribution of velocity $f'(\eta)$, microrotation $g(\eta)$, and temperature $\theta(\eta)$ at a fixed value of $n = 0$ for various physical parameters of interest. The boundary condition $n = 0$ corresponds to the no spin condition, which occurs when the particle density is sufficiently high that the microelements close to the wall are unable to rotate. These results also support the computation for this investigation because they satisfy the boundary condition used.

Figure 1 shows the effect of the Prandtl number on the temperature profile $\theta(0)$. It is observed that as the Prandtl number increases, the temperature profiles rapidly decrease. This behaviour is expected because fluid has high thermal conductivity at lower Pr values and heat diffuse away from the surface faster than at higher Pr values. As a result, as Pr increases, the boundary layer becomes thinner and reducing the temperature.

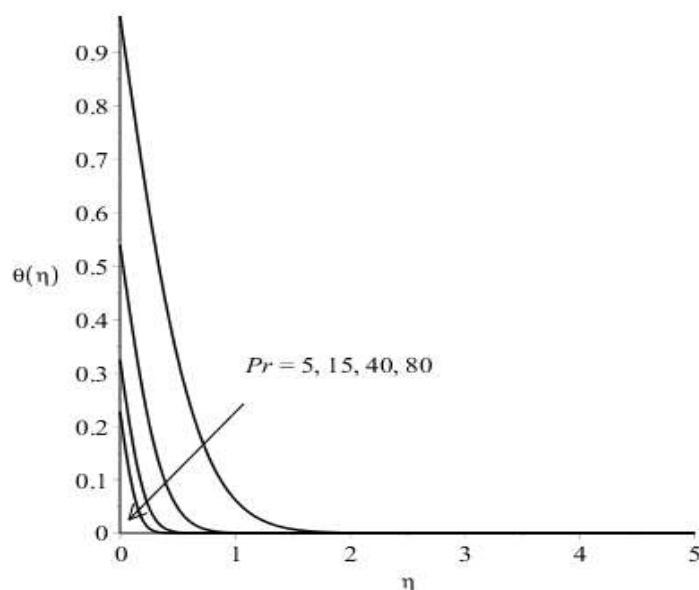


Fig. 1. The temperature profiles for various values of Pr when $K = 0.5, k = 0.2, n = 0, \beta = 0.5, \delta = 0.1, Bi = 1.5, blt = 5$

Figures 2 and 3 depict the distribution of velocity and microrotation for various values of Deborah number. The velocity increases as the Deborah number increases, whereas the temperature profile shows the opposite behaviour. This is in line with the fact that a larger Deborah number corresponds to a longer relaxation time. It is also observed that the microrotation profile decreases near the sheet but twists the pattern where the profiles begin to increase and become zero far away from the sheet. For a fluid with extremely small relaxation time, a very small Deborah number can be obtained and the fluid will act like a solid if the Deborah number is very large.

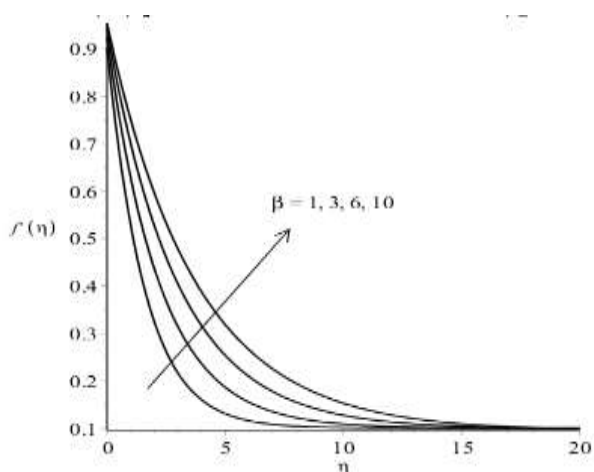


Fig. 2. The velocity profiles for various values of β when $K = 0.5, k = 0.2, n = 0, \delta = 0.1, Bi = 1.5, Pr = 0.71, blt = 20$

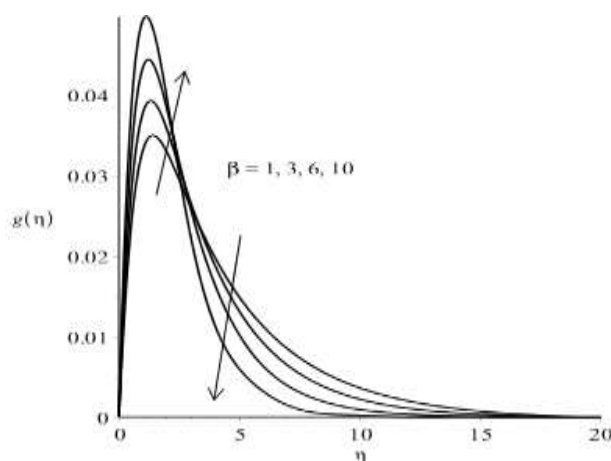


Fig. 3. The microrotation profiles for various values of β when $K = 0.5, k = 0.2, n = 0, \delta = 0.1, Bi = 1.5, Pr = 0.71, blt = 20$

Figures 4 and 5 show the effects of material parameter K on velocity $f'(\eta)$ and microrotation $g(\eta)$. It has been discovered that increasing K causes a decrease in fluid velocity. Meanwhile, for microrotation profiles, the rate of microrotation gradually increases with K until one maximum value and then gradually decreases until it is asymptotically zero.

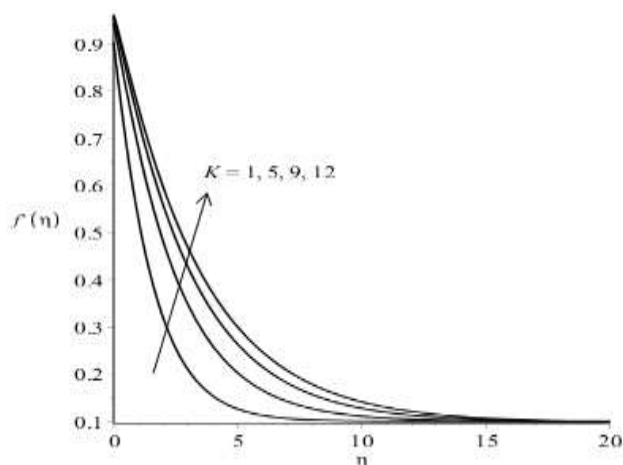


Fig. 4. The velocity profiles for various values of K when $\beta = 0.5, k = 0.2, n = 0, \delta = 0.1, Bi = 1.5, Pr = 0.71, blt = 20$

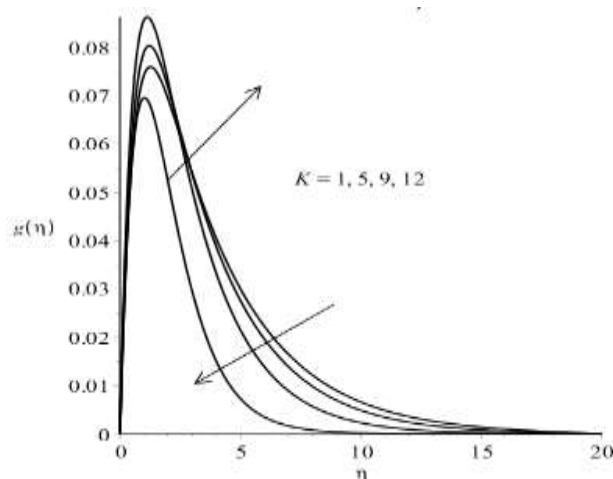


Fig. 5. The microrotation profiles for various values of K when $\beta = 0.5, k = 0.2, n = 0, \delta = 0.1, Bi = 1.5, Pr = 0.71, blt = 20$

Figure 6 indicates that temperature increases for larger thermal Biot number Bi as convective heat transfer coefficient enhances through increasing thermal Biot number Bi . The Biot number is a ratio of the temperature drop in the solid material to the temperature drop in the solid and the fluid. So, for smaller Bi , most of the temperature drop is in the fluid and the solid may be considered isothermal. Therefore, Bi enhances both the temperature field and thermal boundary layer thickness. A lower Bi means that the conductive heat transfer is much faster than the convective heat transfer.

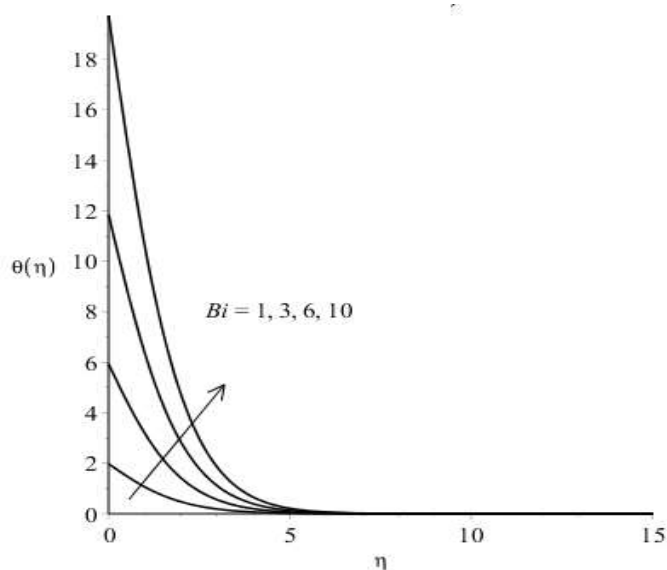


Fig. 6. The temperature profiles for various values of Bi when $\beta = 0.5, k = 0.2, K = 0.5, n = 0, \delta = 0.1, Pr = 0.71, blt = 15$

Figures 7 and 8 show that the microrotation profile and temperature profile is greatly influenced by the velocity slip parameter k . When the values of the velocity slip parameter increase, the temperature profile rises while velocity profile and microrotation profile drop. It is discovered that increasing the velocity slip parameter k increases the heat transfer coefficient which improves the fluid's temperature as well as the thickness of its thermal boundary layer.

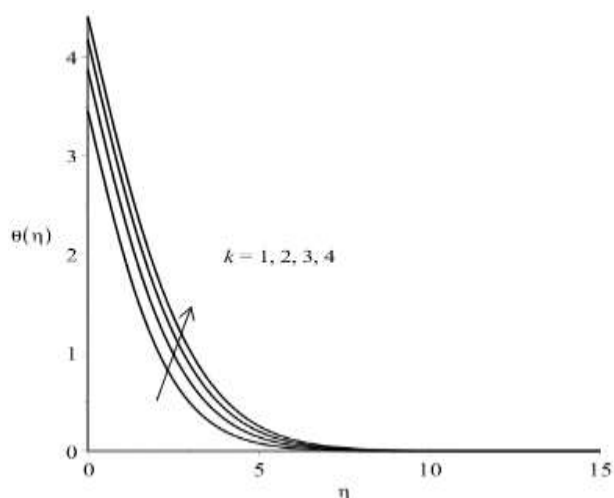


Fig. 7. The temperature profiles for various values of k when $\beta = 0.5, K = 0.5, n = 0, \delta = 0.1, Pr = 0.71, blt = 15, Bi = 1.5$

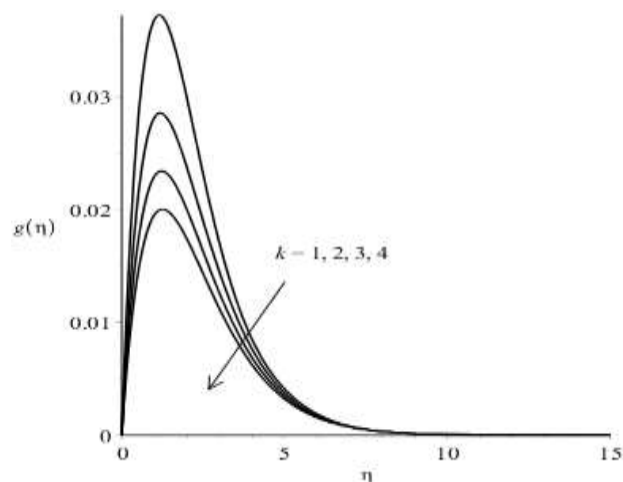


Fig. 8. The microrotation profiles for various values of k when $\beta = 0.5, K = 0.5, n = 0, \delta = 0.1, Pr = 0.71, blt = 15, Bi = 1.5$

Figure 9 shows the distribution of velocity for various values of stretching parameter. The velocity and microrotation are increased as the values of stretching stretch parameter increases while the temperature profile shows the opposite behaviour.

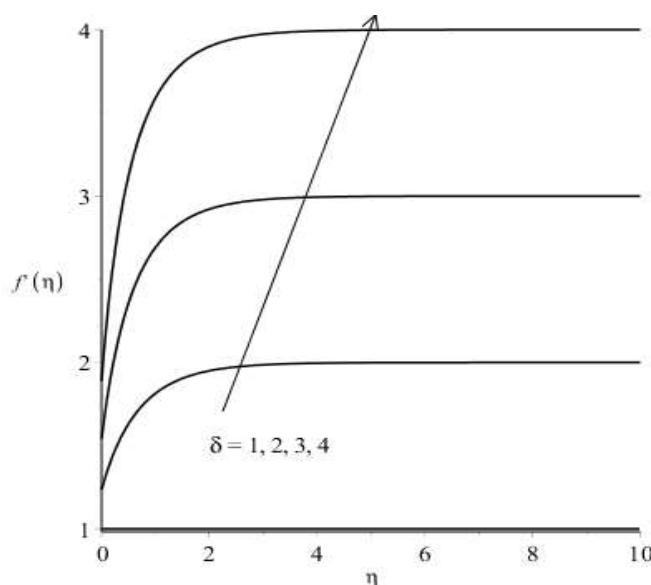


Fig. 9. The velocity profiles for various values of δ when $\beta = 0.5, K = 0.5, n = 0, Pr = 0.71, blt = 15, Bi = 1.5, k = 0.2$

Figure 10 shows the distribution of microrotation for various values of concentration of microelements. In the case of strong concentration, the microelements are not able to rotate near

the walls so it can be seen that the microrotation becomes zero at the plates. This figure shows that increasing the micropolar parameter causes an increase in the thermal boundary layer thickness, which causes the temperature profile to rise, but the increase is not considerable.

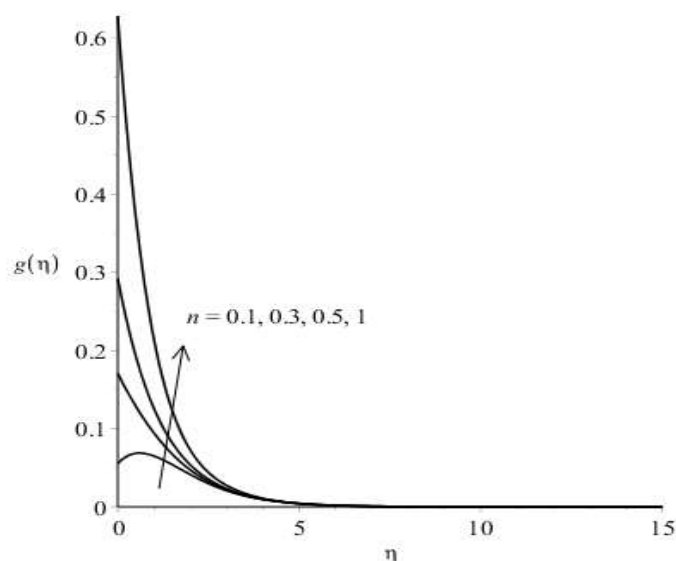


Fig. 10. The microrotation profiles for various values of n when $\beta = 0.5$, $K = 0.5$, $Pr = 0.71$, $blt = 15$, $Bi = 1.5$, $k = 0.2$, $\delta = 0.1$

4. Conclusions

This paper aims to investigate at Jeffrey fluid flow over a stretching sheet with microrotation effect under convective boundary conditions. The partial differential equations of the proposed model are reduced into ordinary differential equations using the similarity transformation variables. The resulting equations have been solved by using the RKF45 method. The numerical algorithm was carried out by using the Maple software. The graph for velocity, microrotation, and temperature profiles is shown against several involved parameters. It is found that the parameters that have been discussed also improved with the addition of Biot number and concentration of microelements. The obtained numerical results can provide the theoretical prediction that may serve as a baseline for fluid flow in engineering applications and other fluid related fields. Note that, the Jeffrey fluid is important in pharmaceuticals, physiology, fibers technology, food products, wire coating, crystal growth and other fields.

Acknowledgement

The authors extend their heartfelt gratitude to Universiti Teknologi MARA (UiTM), Johor Branch Pasir Gudang Campus, for their support. Special appreciation is also conveyed to Universiti Teknologi MARA (UiTM), Terengganu Branch and Universiti Malaysia Pahang Al-Sultan Abdullah for their invaluable guidance and contributions.

References

- [1] Nadeem, Sohail, and Noreen Sher Akbar. "Peristaltic flow of a Jeffrey fluid with variable viscosity in an asymmetric channel." *Zeitschrift für Naturforschung A* 64, no. 11 (2009): 713-722. <https://doi.org/10.1515/zna-2009-1107>
- [2] Khan, Masood, Faiza Iftikhar, and Asia Anjum. "Some unsteady flows of a Jeffrey fluid between two side walls over a plane wall." *Zeitschrift für Naturforschung A* 66, no. 12 (2011): 745-752.

- [3] Hayat, Tasawar, Sabir Ali Shehzad, Muhammad Qasim, and Saleem Obaidat. "Thermal radiation effects on the mixed convection stagnation-point flow in a Jeffery fluid." *Zeitschrift für Naturforschung A* 66, no. 10-11 (2011): 606-614. <https://doi.org/10.5560/zna.2011-0024>
- [4] Hayat, T., Sadia Asad, M. Qasim, and Awatif A. Hendi. "Boundary layer flow of a Jeffrey fluid with convective boundary conditions." *International Journal for Numerical Methods in Fluids* 69, no. 8 (2012): 1350-1362. <https://doi.org/10.1002/flid.2642>
- [5] Akaje, Wasiu, and B. I. Olajuwon. "Impacts of Nonlinear thermal radiation on a stagnation point of an aligned MHD Casson nanofluid flow with Thompson and Troian slip boundary condition." *Journal of Advanced Research in Experimental Fluid Mechanics and Heat Transfer* 6, no. 1 (2021): 1-15.
- [6] Yusefi, Mostafa, Kamyar Shameli, and Siti Nur Amalina Mohamad Sukri. "Magnetic nanoparticles in hyperthermia therapy: a mini-review." *Journal of Research in Nanoscience and Nanotechnology* 2, no. 1 (2021): 51-60. <https://doi.org/10.37934/jrnn.2.1.5160>
- [7] Vajravelu, K., S. Sreenadh, and P. Lakshminarayana. "The influence of heat transfer on peristaltic transport of a Jeffrey fluid in a vertical porous stratum." *Communications in Nonlinear Science and Numerical Simulation* 16, no. 8 (2011): 3107-3125. <https://doi.org/10.1016/j.cnsns.2010.11.001>
- [8] Turkyilmazoglu, M., and I. Pop. "Exact analytical solutions for the flow and heat transfer near the stagnation point on a stretching/shrinking sheet in a Jeffrey fluid." *International Journal of Heat and Mass Transfer* 57, no. 1 (2013): 82-88. <https://doi.org/10.1016/j.ijheatmasstransfer.2012.10.006>
- [9] Mohd Zin, Nor Athirah, Ilyas Khan, and Sharidan Shafie. "Exact and numerical solutions for unsteady heat and mass transfer problem of Jeffrey fluid with MHD and Newtonian heating effects." *Neural Computing and Applications* 30, no. 11 (2018): 3491-3507. <https://doi.org/10.1007/s00521-017-2935-6>
- [10] Eringen, A. Cemal. "Theory of micropolar fluids." *Journal of mathematics and Mechanics* (1966): 1-18. <https://doi.org/10.1512/iumj.1967.16.16001>
- [11] Sandeep, N., and C. Sulochana. "Dual solutions for unsteady mixed convection flow of MHD micropolar fluid over a stretching/shrinking sheet with non-uniform heat source/sink." *Engineering Science and Technology, an International Journal* 18, no. 4 (2015): 738-745. <https://doi.org/10.1016/j.jestch.2015.05.006>
- [12] Rawi, Noraihan Afiqah, Nor Athirah Mohd Zin, Asma Khalid, Mohd Kasim, Abdul Rahman, Zaiton Mat Isa, and Sharidan Shafie. "Numerical solutions for convective boundary layer flow of micropolar Jeffrey fluid with prescribe wall temperature." *Journal of the Indonesian Mathematical Society* 26, no. 3 (2020): 286-298. <https://dx.doi.org/10.22342/jims.26.3.553.286-298>